

# Method for Vector Map Protection based on using of a Watermark Image as a Secondary Carrier

Yuliya Vybornova<sup>1</sup> and Vladislav Sergeev<sup>1,2</sup>

<sup>1</sup>*Department of Geoinformatics and Information Security, Samara National Research University, Moskovskoye Shosse, Samara, Russia*

<sup>2</sup>*Image Processing Systems Institute of RAS – Branch of the FSRC “Crystallography and Photonics” RAS, Samara, Russia*

**Keywords:** Digital Watermarking, Geographic Information Systems, GIS, Vector Map, Raster Image, Discrete Fourier Transform, Pseudorandom Sequences, Data Protection.

**Abstract:** In this paper, we present a study of the watermarking method for vector cartographic data based on a cyclic shift of a polygon vertex list. We propose a method modification to provide an accurate authentication procedure, as well as to increase the method robustness against map contents modification. The main idea of the improved method is to use a noise-like image as a secondary carrier for a watermark, represented in the form of a bit vector. An algorithm for construction of a noise-like image carrying a watermark sequence, as well as an algorithm for extraction of such a sequence, are given. An experimental study explores the information capacity of the carrier image and its robustness against quantization and noise adding, i.e. distortions simulating the embedding into map objects. The efficiency of the method is also demonstrated on real cartographic data. Conclusions comprise optimal parameters for reliable extraction depending on the number of polygons on the vector map.

## 1 INTRODUCTION

The existing methods of active protection (i.e. the protection by using digital watermarking technology) of vector map data are mostly performed by introducing slight (in terms of map accuracy) distortions into the coordinate information of vector objects (Abubahia and Cocea, 2017). Depending on the level of watermark resistance to distortions, these methods are aimed at solving various problems of vector map security.

Methods (Abubahia and Cocea, 2015; Lee and Kwon, 2013; Peng et al., 2015; Wang, Yang and Zhu, 2017; Yan, Zhang and Yang, 2017; Zope-Chaudhari, Venkatachalam and Buddhiraj, 2017) are designed for solving the problem of copyright protection (protection against unauthorized distribution) using the technology of robust watermarks. Methods of protection against modifications are implemented on the basis of semi-fragile (Ren, Wang and Zhu, 2014; Da et al., 2018) and fragile (Wang, Bian and Zhang, 2015) watermarks, which are used to ensure the authenticity and integrity of vector data respectively. Also, one of the common approaches to protect

vector data against changes is the so called "zero-watermarking" technology (Peng and Yue, 2015) which implies constructing a watermark on the basis of the carrier features. Here, the embedding procedure as such is missing: the watermark is necessary only for the verification process. The combined use of different watermarking technologies, which is called "multiple watermarking" (Peng et al., 2017), allows to provide comprehensive protection of vector data from unauthorized distribution and modification.

There are situations where even minor changes introduced into the data are unacceptable. For this reason, another class of vector data protection methods, "reversible watermarking" (Cao, Men and Ji, 2015; Peng, Yan and Long, 2017; Wang, Zhao and Xie, 2016), has emerged, providing the opportunity to restore the coordinate values after the watermark extraction. However, these methods do not demonstrate the required robustness, therefore, map distortions can negatively affect the correct restoration of the original coordinate values.

It should be noted that all the above mentioned methods have the following disadvantages:

- Despite the fact that all conversions are performed with a given accuracy and almost invisible to the legitimate user, any distortion of the map gives an attacker the opportunity to detect the presence of the embedded watermark even without knowing the watermarking scheme, i.e. by using blind steganalysis.

- When embedding and extracting the watermark, a set of map objects must be strictly ordered. Since the location of objects on the map is quite random, there is a need to store extra identifiers for objects or watermark positions.

The embedding approach, we proposed earlier in (Vybornova and Sergeev, 2019), allows to avoid the above disadvantages. First, the method does not imply a change in vertex coordinates: the protective information is embedded into cartographic data by cyclically shifting the list of vertices of each polygon. Secondly, instead of a bit sequence we consider a raster image superimposed on a vector map as a digital watermark, so there is no need to fix the object indexation order when embedding and extraction procedures. Consequently, this approach to vector map protection can form the basis for a whole group of methods, focused on specific tasks, such as copyright, authenticity and integrity protection of map data, as well as localization of unauthorized changes introduced into a vector map.

In this paper, we propose a specific way of using a noise-like image as a secondary carrier for the watermark presented in the conventional form of a bit sequence, and also we explore the issue of the information capacity of such a carrier.

The rest of the paper is organized as follows. In Section 2, the basic approach, which we developed earlier, is presented. Also, this section describes in detail a new enhanced approach. Section 3 comprises experimental research of the proposed method for model and real data. Section 4 provides general conclusions and the main issues of the future work.

## 2 METHODS

### 2.1 Original Watermarking Method for Vector Maps

The basic watermarking method for vector cartographic data, that we proposed in (Vybornova and Sergeev, 2019), is based on the following features of polygonal map objects:

a) all polygons are closed shapes;

b) the polygon vertices are numbered consecutively.

These properties provide the ability to cyclically shift the indices of all vertices in the polygon vertex list, without changing the coordinate values, that is, avoiding the introduction of distortions into the vector map contents.

The first idea of the method (Vybornova and Sergeev, 2019) is that the digital watermark is embedded into data by cyclically shifting the list of vertices of each polygon. For example, to embed one watermark bit into each polygon, a polygon vertex list can be shifted in such a way as to change the first element in the list to either the uppermost (north) or the lowermost (south) vertex, depending on the value of the watermark bit. To embed two watermark bits into the polygon, the leftmost (west) and rightmost (east) vertices should be also taken into consideration. In general, an  $n$ -bit binary number can be embedded into each polygon. It should be noted that for a fixed first vertex of the list, there is an opportunity to embed an additional watermark bit into each polygon by altering the direction of vertex traversal: clockwise or counterclockwise, depending on the bit value.

The second idea of the method is to use a raster image superimposed on a selected fragment of the vector map as a watermark. Certainly, the vector map does not provide an opportunity to place raster data, but its objects (in our case, polygons) can be mapped to the image in such a way as to geometrically coincide with some pixels. The set of pixels, corresponding to polygons, forms an irregular grid, and thus the entire image can be approximately restored by using one of the existing interpolation methods (Vybornova, 2018).

### 2.2 Proposed Enhancement of Original Method

In method (Vybornova and Sergeev, 2019), the raster image itself is used as a robust watermark providing copyright protection for a digital map. Accordingly, the map authentication is performed by visually matching the original watermark with the image restored (usually with large errors) after extracting from the vector map. So, this can be regarded as an obvious limitation on the method applicability.

Developing the basic method, we propose to use a noise-like image as a secondary carrier for the watermark, represented in the form of a bit sequence (Glumov and Mitekin, 2010). This allows to automate the map authentication procedure, since

the watermark sequence can itself carry all the necessary identifying information and its analysis does not require the comparison with the original watermark.

In order to ensure robustness of the embedded bit sequence against image interpolation errors, addition or removal of map objects, geometrical transformations and cropping of the map, and etc., each bit embedded in the carrier image should not correspond to a separate point (pixel) or a local area on the image plane. We propose to embed a bit sequence in the spatial-frequency domain of the carrier image so that each bit is extended on the entire image plane "holographically", i.e. in the form of a two-dimensional sinusoid of the corresponding spatial frequency.

### 2.3 Watermark Image Construction

For simplicity, we assume the carrier image is continuous -  $f_c(t_1, t_2)$ . We also assume it carries a watermark in the form of an arbitrary binary sequence  $S$  of length  $L$ .

We propose to form a two-dimensional spatial spectrum -  $F_c(\omega_1, \omega_2)$  - of an image represented as  $2(L+2)$  two-dimensional unit impulses located in the spectral domain on two rings of different radii:  $r$  and  $r+\Delta r$ , as illustrated in Fig. 1 for one half-plane of the two-dimensional spectrum (because the image is real the second half-plane displays the spectrum symmetrically about the center). In figure 1, unit impulses are indicated with black circles. All but two impulses are located with equal step (angle) starting from the spectrum origin on a ring of smaller or larger radius, depending on the value of the corresponding bit of the watermark sequence. Two impulses located on both rings at the same (e.g. zero) angle indicate the beginning of the sequence.

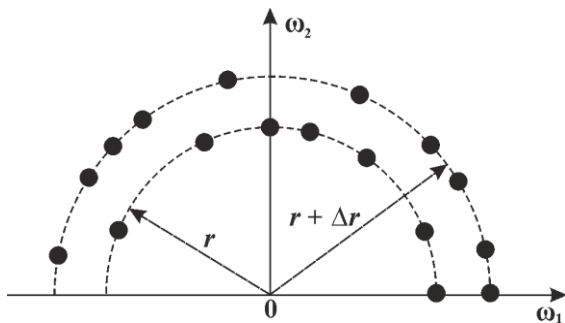


Figure 1: Embedding of a binary sequence into image spectrum.

The resulting spectrum of an image can be described by the formula:

$$\begin{aligned}
 F_c(\omega_1, \omega_2) &= \\
 &= \sum_{l=1}^L \delta(\omega_1 - \rho_l \cos \varphi_l, \omega_2 - \rho_l \sin \varphi_l) + \\
 &+ \delta(\omega_1 - r, \omega_2) + \delta(\omega_1 - r - \Delta r, \omega_2) + \quad (1) \\
 &+ \sum_{l=1}^L \delta(\omega_1 + \rho_l \cos \varphi_l, \omega_2 + \rho_l \sin \varphi_l) + \\
 &+ \delta(\omega_1 + r, \omega_2) + \delta(\omega_1 + r + \Delta r, \omega_2).
 \end{aligned}$$

where  $\rho_l = r + s_l \Delta r$ ,  $\varphi_l = \frac{\pi l}{L+1}$ , and  $\delta(\omega_1, \omega_2)$  is a two-dimensional unit impulse.

To get the two-dimensional image function, we apply the two-dimensional inverse Fourier transform to the spectrum (1):

$$\begin{aligned}
 f_c(t_1, t_2) &= \\
 &= \frac{1}{4\pi^2} \int_{-\infty}^{\infty} \int_{-\infty}^{\infty} F_c(\omega_1, \omega_2) e^{i(\omega_1 t_1 + \omega_2 t_2)} d\omega_1 d\omega_2. \quad (2)
 \end{aligned}$$

By substituting (1) into (2), and taking into account the Euler's formula, we obtain:

$$\begin{aligned}
 f_c(t_1, t_2) &= \frac{1}{2\pi^2} \left\{ \sum_{l=1}^L \cos[(\rho_l \cos \varphi_l) t_1 + \right. \\
 &+ (\rho_l \sin \varphi_l) t_2] + \cos(r t_1) + \cos[(r + \Delta r) t_2] \left. \right\} \quad (3)
 \end{aligned}$$

The above relations describe only the idea of how to embed a binary sequence into a carrier image. In practice, when working with a digital image instead of a continuous spectrum, it is necessary to use a discrete Fourier transform (DFT), taking into account the well-known features of such a conversion: integer arguments in the spatial and spectral domain, periodicity of functions in two dimensions, possible overlap effects, etc. In this case, there are two ways to form a noise-like image, carrying a watermark of size  $N_1 \times N_2$  pixels:

1) By directly using the "discretized" analogue of the formula (3):

$$\begin{aligned}
 f(n_1, n_2) &= \sum_{l=1}^L \cos[2\pi(\frac{\rho_l \cos \varphi_l}{N_1} n_1 + \frac{\rho_l \sin \varphi_l}{N_2} n_2)] + \\
 &+ \cos(\frac{2\pi r}{N_1} n_1) + \cos[\frac{2\pi(r + \Delta r)}{N_2} n_2],
 \end{aligned}$$

where  $n_1, n_2$  are the integer arguments of the digital image,  $0 \leq n_1 \leq N_1 - 1, 0 \leq n_2 \leq N_2 - 1$ .

2) By directly using the "discretized" analogue of unit impulse delta function, called unit sample function. Unit samples are arranged on two rings in two-dimensional discrete spectral domain as described above, and then the resulting image can be obtained by using the inverse DFT.

For small lengths of sequences, the first method may be computationally more efficient. Contrariwise, when lengths are large enough, the second method may perform in a better way.

It should be noted that due to the spectrum discreteness, the coordinates of unit samples, i.e. magnitudes  $\rho_1 \cos \varphi_1, \rho_1 \sin \varphi_1, r, (r + \Delta r)$  should be rounded to integer values and, therefore, may overlap when arranging on the rings. Thus, the DFT dimensions and the radii  $r, (r + \Delta r)$  must be sufficiently large, so that rounding errors could not affect the watermark extraction.

As the last step of constructing the carrier image, the values of its pixels can be normalized to a standard range, for example,  $[0, 255]$ :

$$f_{255}(n_1, n_2) = 255 \frac{f(n_1, n_2) - \min_{n_1, n_2} f(n_1, n_2)}{\max_{n_1, n_2} f(n_1, n_2) - \min_{n_1, n_2} f(n_1, n_2)}$$

An example of the resulting noise-like image with embedded watermark sequence corresponding to spectrum in Figure 1 is shown in Figure 2.

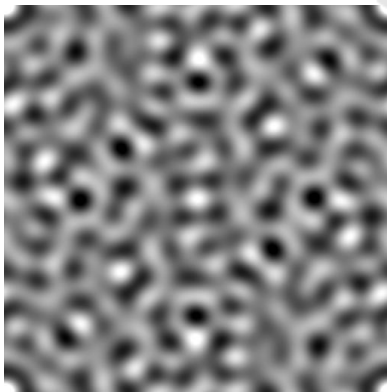


Figure 2: Example of noise-like image carrying the watermark sequence ( $N_1 = N_2 = 512, r = 8, \Delta r = 4, L = 15, S = \{101101001011101\}$ ).

## 2.4 Watermark Extraction

The extraction of a sequence from an image approximately (with interpolation) reconstructed

from a vector map consists of the following obvious steps:

- calculation of a two-dimensional discrete spectrum of the image (using DFT);
- detection of spectral components with a large amplitude (impulses) and determination of their coordinates;
- detection of the fact of watermark presence, i.e. the fact that the impulses are located on two concentric rings in the spectral plane; estimation of the radii of these rings;
- search of the sequence beginning key, i.e. a pair of impulses located at the same angle to the spectrum origin;
- reading of the watermark sequence bits clockwise or counterclockwise starting from the sequence beginning key.

The proposed method of watermark construction (in the form of impulses on circles in the spectral plane), together with the extraction procedure described above, ensures the watermark robustness against the main geometric deformations of the image and, accordingly, of the vector map into which this image is embedded: scaling, rotation, translation and cropping.

## 3 EXPERIMENTAL RESULTS AND DISCUSSION

To investigate the potential use of a noise-like image embedded into the vector map as a secondary container for the watermark presented in the form of a bit sequence, we have conducted two computational experiments.

In all experiments, digital images of size  $N_1 \times N_2 = 512 \times 512$  pixels are generated. Bit sequences are embedded into rings of radii  $r$  and  $(r + \Delta r)$  in the discrete spectrum domain of the image (for certainty, it is assumed that  $\Delta r = 4$ , since due to the discreteness of the bitmap it is the minimum acceptable value). The "low-frequency" ( $r = 10, 50$ ) and "mid-frequency" ( $r = 60, 100$ ) noise-like images are considered.

The lengths of the bit sequences are ranged from  $10 \leq L \leq 100$ . For each combination of parameters, 100 watermark sequence implementations are generated. The values of sequence bits are obtained using a random number generator as equiprobable and independent in total.

Interpolation of an image extracted from a vector map is performed using the nearest neighbor method

based on a triangulated irregular network (Vybornova, 2018).

Spectral impulses are determined using a simple rule:

$$F(k_1, k_2) > \frac{1}{2} \max_{\substack{k_1, k_2 \\ (k_1, k_2) \neq (0,0)}} |F(k_1, k_2)|$$

where  $F(k_1, k_2)$  is the image DFT,  $k_1, k_2$  are the integer arguments of the discrete spectrum ( $0 \leq k_1 \leq N_1 - 1, 0 \leq k_2 \leq N_2 - 1$ ).

### 3.1 Experiment 1

Obviously, the main sources of errors during the reconstruction of a carrier image from a vector map and, consequently, errors during the bit sequence extraction, are:

- the image is extracted from the map as a set of spaced pixels corresponding to the polygonal map objects;
- extracted pixels are quantized due to the fact that only few binary digits can be embedded into each polygon.

To evaluate the effect of these distortions on the watermark sequence, we conducted the following computational experiment.  $K$  pixels of the generated noise-like image are selected randomly (independently and equally likely for each coordinate). Each pixel is quantized to a  $b$ -bit binary number (i.e. into  $2^b$  levels). Next, the image is interpolated and attempt to extract the watermark sequence is performed.

As an indicator of the watermark sequence integrity, the experimentally estimated probability of its correct extraction,  $P$ , depending on the number of reference pixels  $K$ , is considered. Estimation of the extraction probability is calculated for the sample of 100 images.

The variable values are: radius  $r$ , bit depth (i.e. number of bits per pixel  $b$ ), and sequence length  $L$ . The minimum values of  $r$  are established experimentally and can approximately be described by the formula:

$$r \geq 0,36L .$$

Figure 3 shows the dependence of the extraction probability on the number of polygons with varying values of bit depth for the following cases: a)  $L = 10$ , b)  $L = 50$ , c)  $L = 100$  (in each case, the radii are selected in such a way as to provide the most

accurate extraction, i.e. they are assigned the lowest acceptable values).

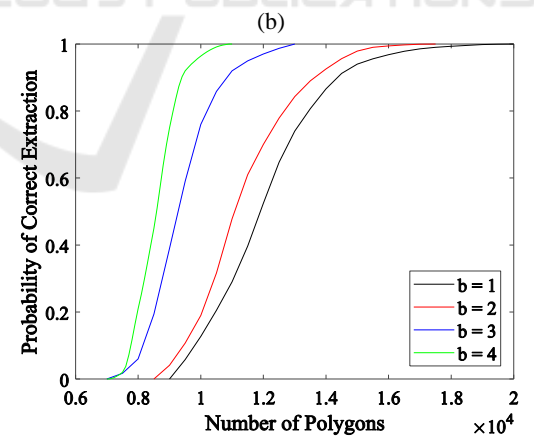
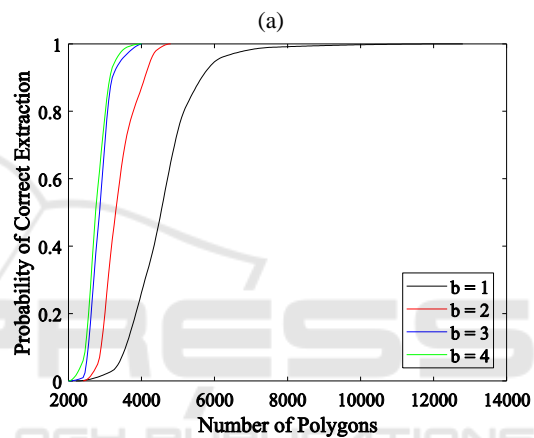
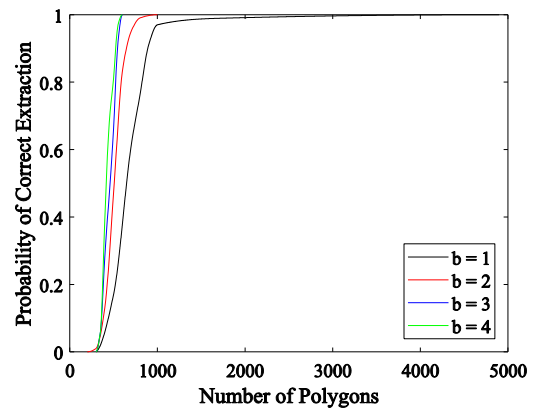
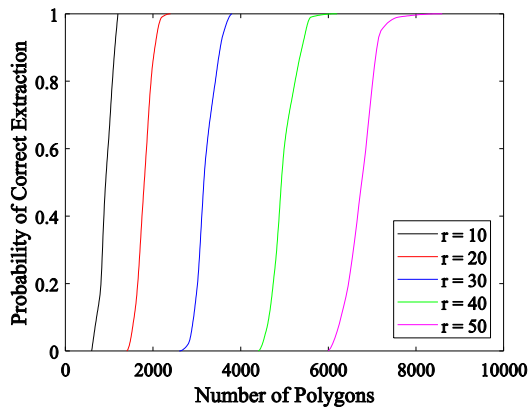


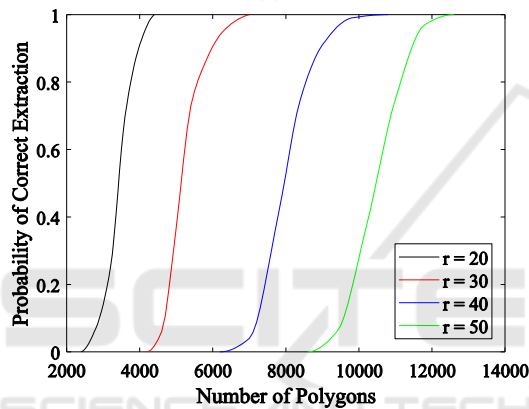
Figure 3: Dependence of the extraction probability on the number of polygons with variable values of bit depth  $b$  for a)  $L = 10, r = 10$ ; b)  $L = 50, r = 20$ ; c)  $L = 100, r = 40$ .

Figure 4 shows the dependence of the extraction probability on the number of polygons with varying values of the radii for the following cases: a)  $L = 10$ ,

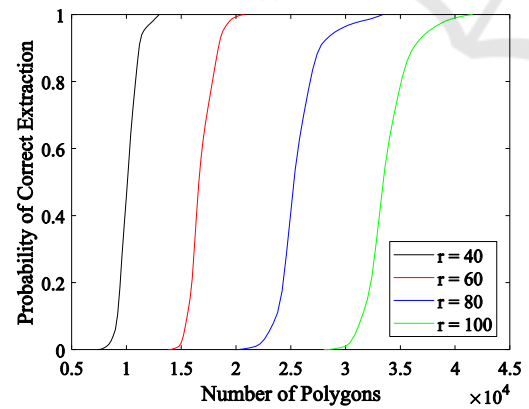
b)  $L = 50$ , c)  $L = 100$  (the bit value in this case is fixed as  $b = 3$ )



(a)



(b)



(c)

Figure 4: The dependence of the extraction probability on the number of polygons with varying values of the radii for a)  $L = 10$ ,  $b = 3$ ; b)  $L = 50$ ,  $b = 3$ ; c)  $L = 100$ ,  $b = 3$ .

Some obvious conclusions follow from the presented results.

The more objects on the map (pixels corresponding to polygons), the higher the probability of correct extraction. At the same time, the longer the watermark sequence, the higher the requirements for the number of objects needed for extraction.

The quality of the extraction increases with an increase in the bit depth of the pixels corresponding to the map objects. It also looks natural, since an increase in the bit depth reduces the pixel quantization noise and, consequently, the error of the carrier image reconstruction decreases. However, when setting the bit depth value higher than  $b = 3$ , we see almost no effect of improving the quality. Moreover, in practical applications it is difficult to implement persistent high bit depth due to the fact that on the real map simple polygons (mostly, quadrangles) dominate: therefore, no more than three-digit binary numbers can be embedded: two digits by setting the first vertex in the polygon vertex list, and one of digit - by altering the direction of vertex traversal.

For a fixed length of the bit sequence, the extraction quality is higher, the smaller the  $r$ , i.e. the lower the frequency of the carrier image. On the other hand, the minimum possible value of this parameter is limited by the discreteness of the two-dimensional image spectrum, namely, its ring into which a sequence of length  $L$  is embedded.

Figure 5 shows the dependence of the watermark image capacity  $b \times L$  on the number of polygons for a fixed values of the achievable probability.

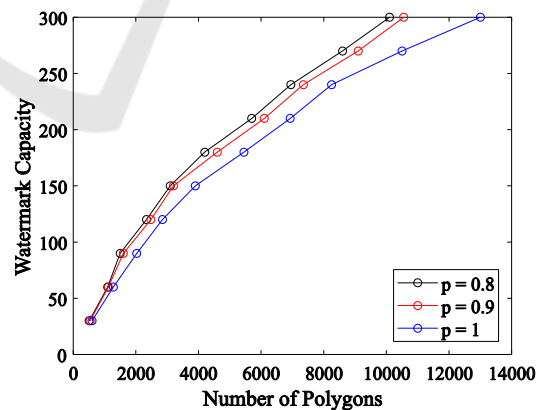


Figure 5: Dependence of carrier image capacity on the number of polygons for various probabilities.

### 3.2 Experiment 2

In the previous experiment, the map watermarking procedure is simulated, but the embedding into real data is not performed. To confirm the performance

of the proposed method for real vector cartographic data, we have conducted a second experiment using a fragment of the urban development map containing 9327 polygons (Figure 6). The quantized values of the corresponding pixels were embedded into each polygon of the map and then extracted.



Figure 6: Carrier map.

As already mentioned, the proposed map watermarking method has features that in one way or another influence the extraction of the binary vector watermark hidden in the noise-like image:

- 1) the noise-like image extracted from the map forms an irregular grid over which interpolation is performed.
- 2) despite the fact that when embedding we set pixel values quantized by a given level, when extraction these values can be rounded, because to embed a  $b$ -bit number into a polygon without errors, this polygon should have  $2^{b-1}$  vertices (obviously, this condition may not be met).

Consequently, in addition to confirmation of the method applicability on real data, this experiment is aimed at the qualitative assessment of the effect arising from errors introduced by such data regarding the model case presented in the previous experiment.

When modeling data from experiment 1, interpolation is performed on uniformly scattered points, and quantization is carried out strictly at a given level. Thus, in experiment 2 we investigate the probabilities of the correct extraction from noise-like images of three types at once:

- 1) The ideal case (model data from experiment 1). Interpolation is performed using a mask with evenly scattered 9327 points superimposed on noise-like images quantized at a given level.

- 2) Interpolation is performed on an irregular grid of 9327 pixels extracted from a map (Figure 7) superimposed on noise-like images quantized at a given level. This data allow us to trace how the unevenness of the grid affects the result of interpolation and the result of extraction in general.

- 3) Data extracted from the map. This data allow us to trace how the unevenness of the number of polygon vertices affects the result of extraction.

To calculate the probabilities of correct extraction, the experiment is conducted on samples of size 100 for  $L = \overline{10,100}$  (in each case, radii are assigned minimum acceptable values).



Figure 7: Non-uniform interpolation grid.

The dependence of the extraction probability on the length of the bit sequence with varying values of  $b$  are shown in Figure 8.

For  $b = 1, 2$ , the result of the real data extraction error coincides with errors introduced by interpolation on irregular grid. For  $b \geq 3$ , when extraction from real data, rounding errors occur, as discussed above.

The dependence of the extraction probability on the number of image quantization levels with varying values of the sequence length are shown in Figure 9.

The findings of experiment 1 tell us that the quality of extraction is higher, the greater the  $b$ . On real data, the statement remains true only for  $b = 1, 2, 3, 4$ . The larger  $L$ , the greater the drop in quality when  $b > 4$ . When  $b = 8$ , extraction is not possible for any  $L$ .

The results obtained for real map data are mostly influenced from uneven distribution of the number of vertices in each polygon. Figure 10 shows the statistics on the number of vertices for the map from Figure 6.

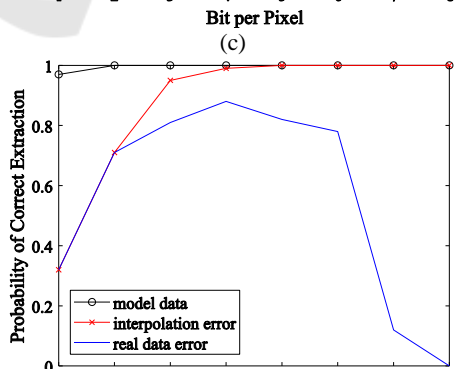
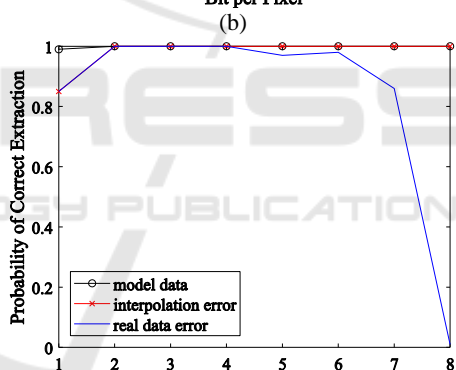
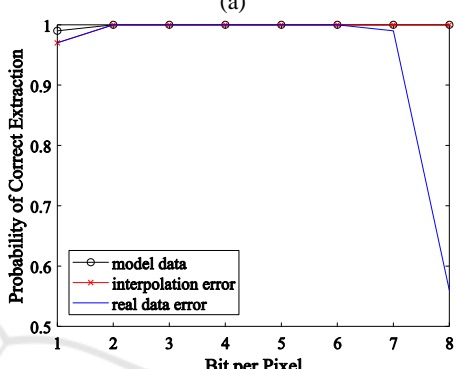
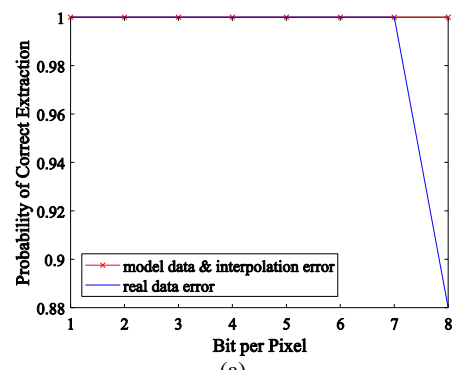
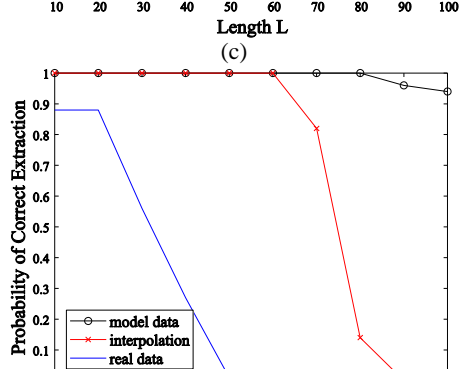
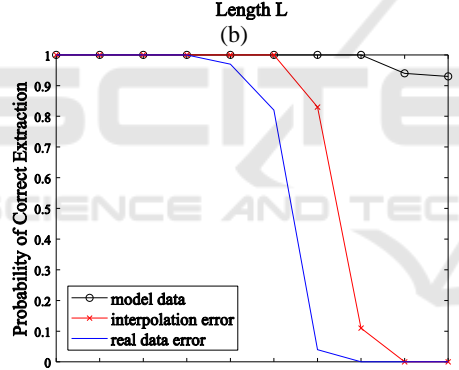
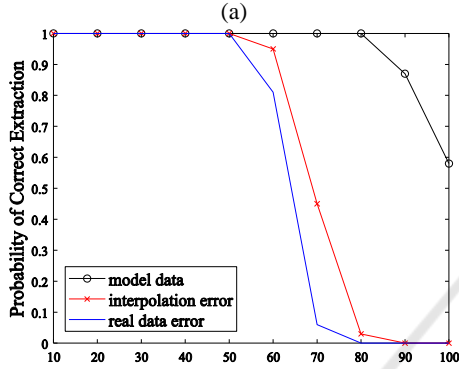
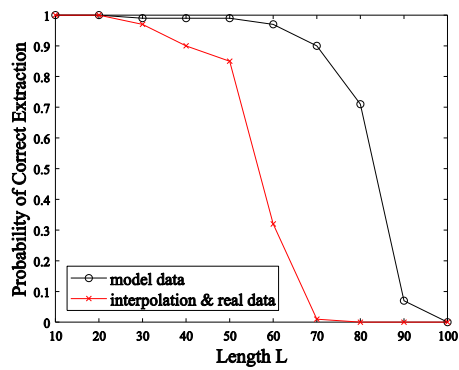


Figure 8: The dependence of the extraction probability on the sequence length for a)  $b = 1$ ; b)  $b = 3$ ; c)  $b = 5$ ; d)  $b = 8$ .

Figure 9: The dependence of extraction probability on the number of image quantization levels for a)  $L = 10$ ; b)  $L = 30$ ; c)  $L = 50$ ; d)  $L = 60$ ; e)  $L = 70$ ; f)  $L = 80$ .

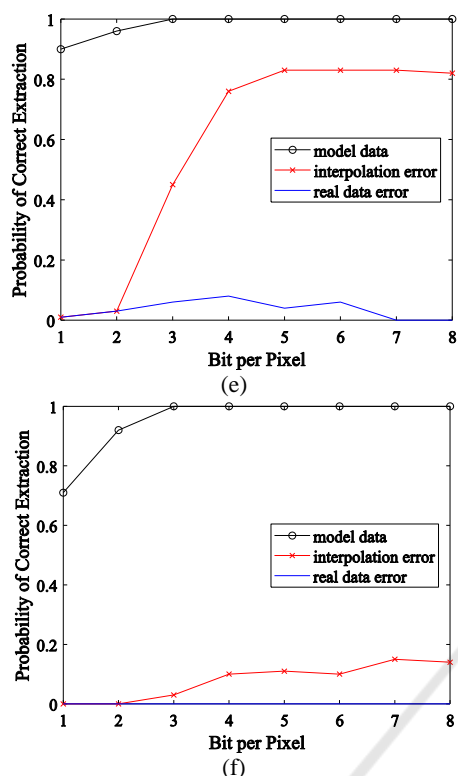


Figure 9: The dependence of extraction probability on the number of image quantization levels for a)  $L = 10$ ; b)  $L = 30$ ; c)  $L = 50$ ; d)  $L = 60$ ; e)  $L = 70$ ; f)  $L = 80$  (cont.).

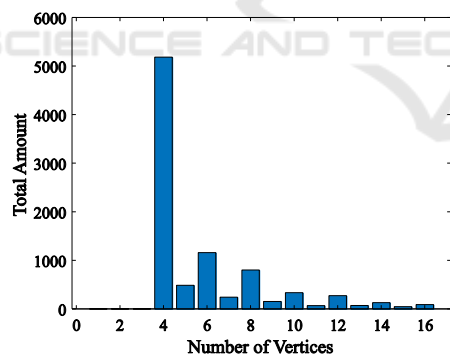


Figure 10: The distribution of the number of vertices for a fragment of urban development map.

Embedding of a  $b$ -bit number into a polygon can be performed with no errors, if the polygon consists of at least  $2^{b-1}$  vertices. For example, to embed a 3-bit number, we should take a polygon of 4 vertices. Such polygons are most likely for maps representing buildings. Embedding of 5 bits requires 16 vertices, which is unlikely for the type of vector maps considered in this paper.

## 4 CONCLUSIONS

In this paper, we present a study of the watermarking method for vector cartographic data based on a cyclic shift of a polygon vertex list. We propose a method modification to provide an accurate authentication procedure, as well as to increase the method robustness against map contents modification. The main idea of the improved method is to use a noise-like image as a secondary carrier for a watermark, represented in the form of a bit vector. An algorithm for construction of a noise-like image carrying a watermark sequence, as well as an algorithm for extraction of such a sequence, are given. An experimental study explores the information capacity of the carrier image and its robustness against quantization and noise adding, i.e. distortions simulating the embedding into map objects. The efficiency of the method is also demonstrated on real cartographic data. Conclusions comprise optimal parameters for reliable extraction depending on the number of polygons on the vector map.

Future work is supposed to be directed towards the following issues:

- 1) a development of computationally efficient and accurate interpolation methods for restoring the undefined pixels on irregular grid;
- 2) a study on the watermark robustness against geometrical transformations and operations changing the map contents, such as simplification (vertex removal), interpolation (vertex addition), object addition / removal, and layer removal;
- 3) a development of methods for increasing the watermark robustness against various types of attacks on vector map data.

## ACKNOWLEDGEMENTS

This work is supported by Russian Foundation for Basic Research (grant № 19-07-00474 A).

## REFERENCES

Abubahia, A. and Cocea, M. (2017). Advancements in GIS map copyright protection schemes - a critical review. *Multimedia Tools and Applications*, 76(10) . – pp. 12205-12231.

Abubahia, A. and Cocea, M. (2015). A clustering approach for protecting GIS vector data. In: *Advanced*

- Information Systems Engineering: 27th International Conference*. pp. 133-147.
- Cao, L., Men, C. and Ji, R. (2015). High-capacity reversible watermarking scheme of 2D-vector data. *Signal, Image and Video Processing*, 9. –pp. 1387–1394.
- Da, Q., Sun, J., Zhang, L., Kou, L. Wang, W. Han, Q. and Zhou, R. (2018). A Novel Hybrid Information Security Scheme for 2D Vector Map. In: *Mobile Networks and Applications*. pp. 1-9.
- Glumov, N.I. and Mitekin, V.A. (2010). The new blockwise algorithm for large-scale images robust watermarking. In: *Proceedings of International Conference on Pattern Recognition*. pp. 1453-1456.
- Lee, S.H. and Kwon, K.R. (2013). Vector watermarking scheme for GIS vector map management. *Multimedia Tools and Applications*, 63(3). – pp. 757-790.
- Peng, F., Yan, Z.J. and Long, M. (2017). A Reversible Watermarking for 2D Vector Map Based on Triple Differences Expansion and Reversible Contrast Mapping. In: *International Conference on Security, Privacy and Anonymity in Computation, Communication and Storage*. pp. 147-158.
- Peng, Y. and Yue, M. (2015). A Zero-Watermarking Scheme for Vector Map Based on Feature Vertex Distance Ratio. *Journal of Electrical and Computer Engineering*, 2015. pp. 1-6.
- Peng, Y., Lan, H., Yue, M. and Xue, Y. (2017). Multipurpose watermarking for vector map protection and authentication. *Multimedia Tools and Applications*, 77(1). – pp. 1-21.
- Peng, Z., Yue, M., Wu, X. and Peng, Y. (2015). Blind watermarking scheme for polylines in vector geospatial data. *Multimedia Tools And Applications*, 74. – pp. 11721-11739.
- Ren, N., Wang, Q. and Zhu, C. (2014). Selective authentication algorithm based on semi-fragile watermarking for vector geographical data In: *22nd International Conference on Geoinformatics*. pp. 1-6.
- Vybornova, Y.D. (2018). Application of spatial interpolation methods for restoration of partially defined images. *CEUR Workshop Proceedings*, 2210. – pp. 89-95.
- Vybornova, Y.D. and Sergeev V.V. (2019). A New Watermarking Method for Vector Map Data. In: *Proceedings of SPIE 11041, Eleventh International Conference on Machine Vision (ICMV 2018)*. pp. 1104111 (1-8).
- Wang, N., Bian, J. and Zhang, H. (2015). RST Invariant Fragile Watermarking for 2D Vector Map Authentication. *International Journal of Multimedia and Ubiquitous Engineering*, 10(4). – pp. 155-172.
- Wang, N., Zhao, X. and Xie, C. (2016). RST Invariant Reversible Watermarking for 2D Vector Map. *International Journal of Multimedia and Ubiquitous Engineering*, 11(2). – pp. 265-276.
- Wang, Y., Yang, C. and Zhu, C. (2017). A multiple watermarking algorithm for vector geographic data based on coordinate mapping and domain subdivision. In: *Multimedia Tools And Applications*. pp. 1–19.
- Yan, H., Zhang, L. and Yang, W. (2017). A normalization-based watermarking scheme for 2D vector map data. *Earth Science Informatics*, 10(4). – pp. 471–481.
- Zope-Chaudhari, S., Venkatachalam, P. and Buddhiraj, K. (2017). Copyright protection of vector data using vector watermark. In: *Geoscience and Remote Sensing Symposium*. pp. 6110-6113.